

RESEARCH PAPER

## Comparative Morphological Study and Evolution of the Silicon Surface Nanostructures: A Time Study of the Transformation from DC Plasma Nanopins to Chemical Etching Nanopyramids

Rudainah Ali Lateef <sup>1\*</sup>, Falih Hamzah Edan <sup>2</sup>, Olfat Ahmed Mahmood <sup>1</sup>, Intessar K. Abd <sup>3</sup>, Muhsin J. Jweeg <sup>4</sup>, Farkad Ali Lattieff <sup>5</sup>

<sup>1</sup> College of Science, University of Diyala, Diyala, Iraq

<sup>2</sup> URUK University, Iraq

<sup>3</sup> College of Education for pure Science, University of Diyala, Diyala, Iraq

<sup>4</sup> Al-Farahidi University, Baghdad, Iraq

<sup>5</sup> College of Engineering, University of Baghdad, Baghdad, Iraq

### ARTICLE INFO

#### Article History:

Received 27 December 2025

Accepted 23 March 2026

Published 01 April 2026

#### Keywords:

Atomic force microscopy

Bradley-Harper theory

Chemical etching

Plasma jet (DC jet)

Silicon etching

Surface roughness

### ABSTRACT

The present comparative study on the morphological evolution of silicon (Si) surfaces generated by two different nanoetching methods: the DC jet plasma physical etching and the wet chemical etching with potassium hydroxide (KOH), with respect to the processing time (1, 2 and 3 min). The obtained surfaces were characterized by atomic force microscopy (AFM) and quantitatively analysed following the international area roughness standards (ISO 25178). The results showed that plasma etching is based on a nonlinear mechanism according to the Bradley-Harper theory and the sharpness of the nanostructures reached a maximum at 2 min before the start of ion polishing at 3 min. Chemical etching results in stable and uniform growth of nanopyramids with geometric dimensions and roughness increasing gradually with time due to anisotropic etching. The study reveals that plasma etching is best suited to produce sharp, isolated needle-like peaks in record time and KOH etching results in surfaces with a homogenous geometric distribution and stable functional surface area. These results provide a framework for nanosurface engineering and the selection of the best etching method based on the topographic requirements for advanced electronic and optical applications.

### How to cite this article

Ali Lateef R, Hamzah Edan F, Ahmed Mahmood O, et al. Comparative Morphological Study and Evolution of the Silicon Surface Nanostructures: A Time Study of the Transformation from DC Plasma Nanopins to Chemical Etching Nanopyramids. J Nanostruct, 2026; 16(2):2179-2190. DOI: 10.22052/JNS.2026.02.063

### INTRODUCTION

Nanosurface engineering of semiconductors, especially Si, is an important foundation stone for the development of next generation optoelectronic devices and microelectromechanical systems (MEMS) [1]. The move from conventional flat surfaces to three-dimensional nanostructures

gives vast possibilities to tune the physical and chemical properties of the material as the rise of the surface-to-volume ratio results in extremely enhanced surface-to-environment interaction [2, 3]. In this context, plasma technologies, particularly DC plasma jet systems have emerged as strategic tools for the fabrication of these nanostructures

\* Corresponding Author Email: rudainah@uodiyala.edu.iq



This work is licensed under the Creative Commons Attribution 4.0 International License.

To view a copy of this license, visit <http://creativecommons.org/licenses/by/4.0/>.

due to their ability to offer high ionic energies and better etching rates than conventional chemical methods [4]. In plasma etching, the mechanism is complex and involves physical ion sputtering. The final surface morphology is determined by the dynamic balance between the induced roughening and the diffusion-driven smoothing [5]. The most accepted mathematical model for this development is the Bradley-Harper Theory, which states that the surface instability and formation of nanostructures depend critically on the energy of the incident ions and the exposure time [6, 7]. However, there is still a research gap that needs to be addressed to have the ability to control the formation of nanopikes and their statistical distribution by DC jet plasma, despite the growing amount of knowledge in this field, especially if we want to correlate these advanced topographic properties to specific functional applications [8,9].

The most exciting aspect of these nanostructures is their outstanding performances in gas sensing applications. The electric field is concentrated at high concentrations in the “hotspots” formed by structures with high statistical parameters, such as kurtosis ( $k_u$ ) and symmetry ( $S_k$ ), promoting molecular adsorption and accelerating charge transfer between the gas and the surface [10, 11]. This physical behaviour is the cornerstone to develop highly sensitive and selective gas sensors at room temperature, which is a major technical challenge in environmental and industrial sensing [12,13].

This study aims to systematically analyse the evolution of silicon surface morphology under the argon plasma for time periods from one to three minutes. This work is based on the ISO 25178 standards for quantitative analysis of the surface roughness with a focus on the morphological transition from sharp peaks to ion-polished surfaces. The work also provides a new physical insight relating etching time with improved performance of gas sensors, aiding in the development of new fabrication standards for silicon based nanosensor platforms with unprecedented performance parameters [14, 15]. Based on the research gap identified in previous studies, this research aims to investigate the dynamic effect of wet chemical etching time using potassium hydroxide (KOH) and plasma etching on the micromorphology and surface topography of silicon at very short times. The results presented show a detailed analysis of the silicon surface after one, two and three minutes of argon plasma etching with DC Jet technology and chemical etching. The data were acquired by atomic force microscopy (AFM) and analysed using the Mountains SPIP software.

This mechanism is based on transfer of mechanical momentum from accelerated ions to surface silicon atoms. If the energy of the incident ion is greater than the binding energy at the surface, the silicon atoms are ejected mechanically [16]. This process allows for anisotropic etching, which leads to highly accurate pattern transfer at

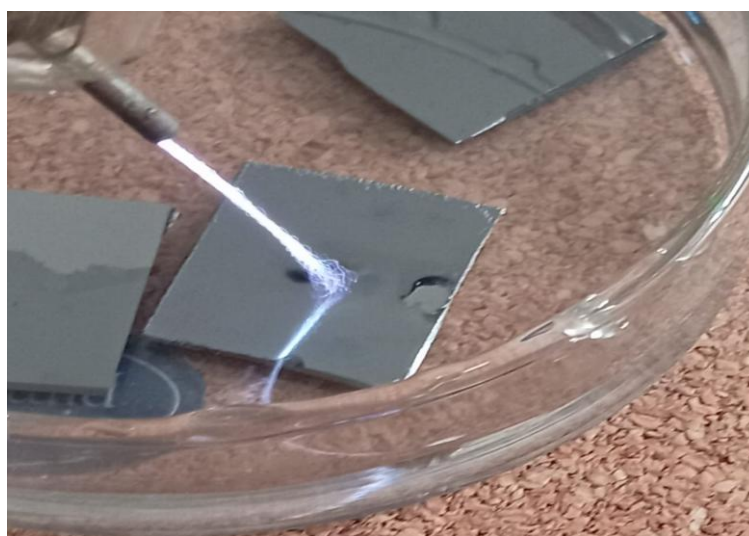


Fig. 1. Silicon Drilling using plasma DC.

the nanoscale. However, heavy ion bombardment can introduce defects in the Si crystal lattice and thus the bias voltage should be carefully balanced [17]. In dc plasma systems, etching is accomplished by creating a strong electric field between two electrodes in a low pressure gaseous environment. If enough voltage is applied, the gas (for example, argon) ionises because the electrons hit the neutral atoms, forming a plasma of positive ions and free electrons [18]. These ions acquire high kinetic energy in the cathode fall zone where they are steered to the silicon substrate placed on the cathode. This process is described by Paschen law, which relates the breakdown voltage to the gas pressure and the distance between the electrodes [19].

Chemical etching is based on spontaneous surface-chemical interactions (with active gas in plasma or liquid solutions) instead of physical

etching. The process involves three basic steps: Adsorption: gathering of reactant molecules on a surface; Surface reaction: cleavage of Si-Si bonds, formation of compounds by dry etching or wet etching; Desorption: loss of products from the surface by volatilisation or dissolution [20]. Chemical etching is highly selective, etching silicon without affecting the mask layers, but tends to be isotropic [21].

**MATERIALS AND METHODS**

*Plasma Drilling*

The bottle features an argon gas which is a major component of the plasma experimental setup that we used in this investigation. A high voltage DC power supply of about 12 kV. The design of a flow meter included calibrations for one for five L/minuet. In this work, argon intake for plate was controlled using a calibration rate of 2 litres

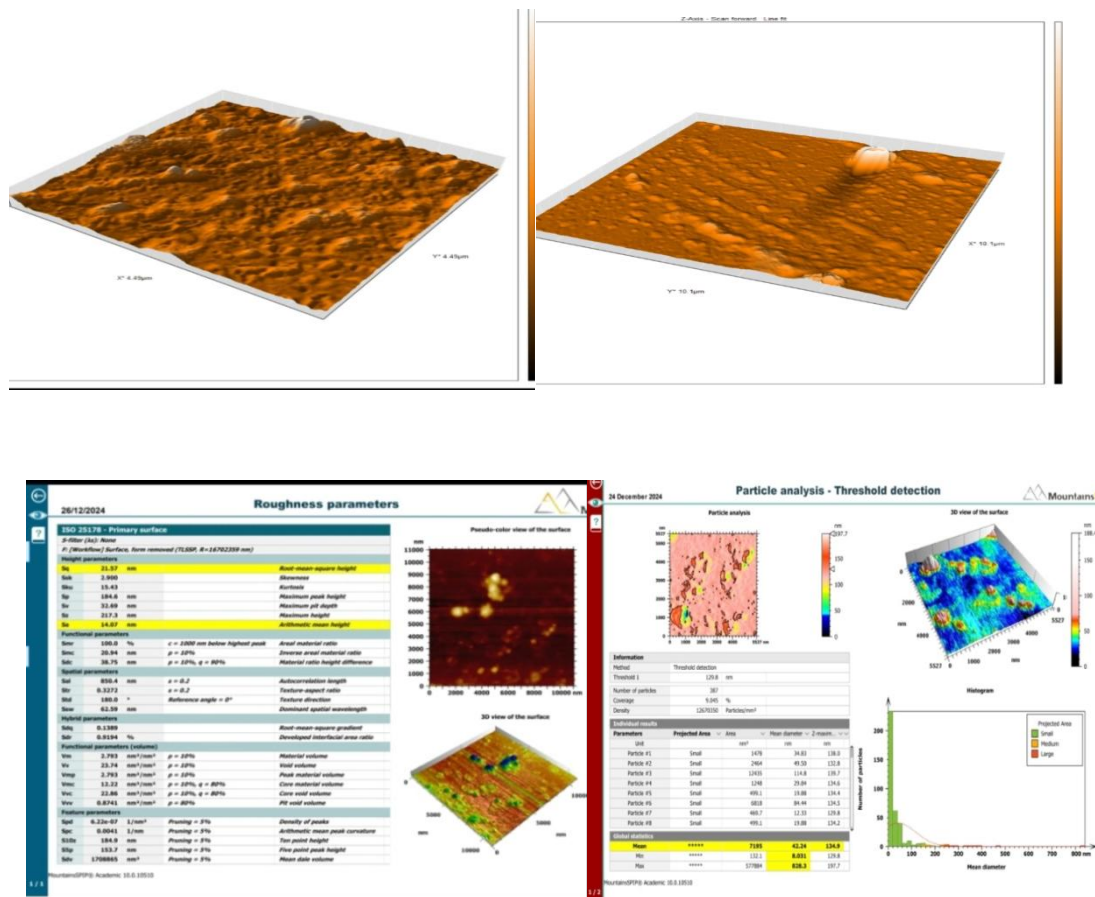


Fig. 2. Topographic characterization and size distribution of nanoparticles on the silicon surface after 1 minutes of plasma etching.

per minute. 1 cm above the liquid is connected to the anode end of the power source. Gas passes through a 1 mm-diameter needle. A conductive tape 6 cm long and 2 cm wide that sticks to the cathode inside the aqueous solution and has a flat tip of 1 x 1 cm at the end. A moveable sample holder that can accommodate different phases. 3. An electrical connection with electrodes attached to gas and liquid. 4. A power source.

**Chemical Etching**

A solution with certain proportions was placed in a glass vessel on a previously prepared piece of silicone, which was purified from impurities. It was allowed to remain for a minute, and the same thing was done with a second piece for two minutes, and a third piece for three minutes. The material was washed with deionised water after the reaction time to quench the reaction.

**RESULTS AND DISCUSSION**

In Fig. 2, three-dimensional atomic force microscopy (AFM) images demonstrate dramatic change of the silicon surface topography after the exposure to the argon plasma (DC jet) for one minute. These modifications are attributed to physical ion sputtering where the accelerated positive argon ions transfer their kinetic energy to the surface silicon atoms, causing displacement and formation of random nanostructures. Microscopic scan shows big protrusions dispersed all over the surface, which indicates that the etching process was not completely homogeneous, as common behaviour when using inert gas plasmas during short periods of time

Average roughness aS, qS. The value of aS was about 14.07 nm. This result is in agreement with the study of Gabor et al [22] on early ion etching of silicon. They observed that the initial few minutes

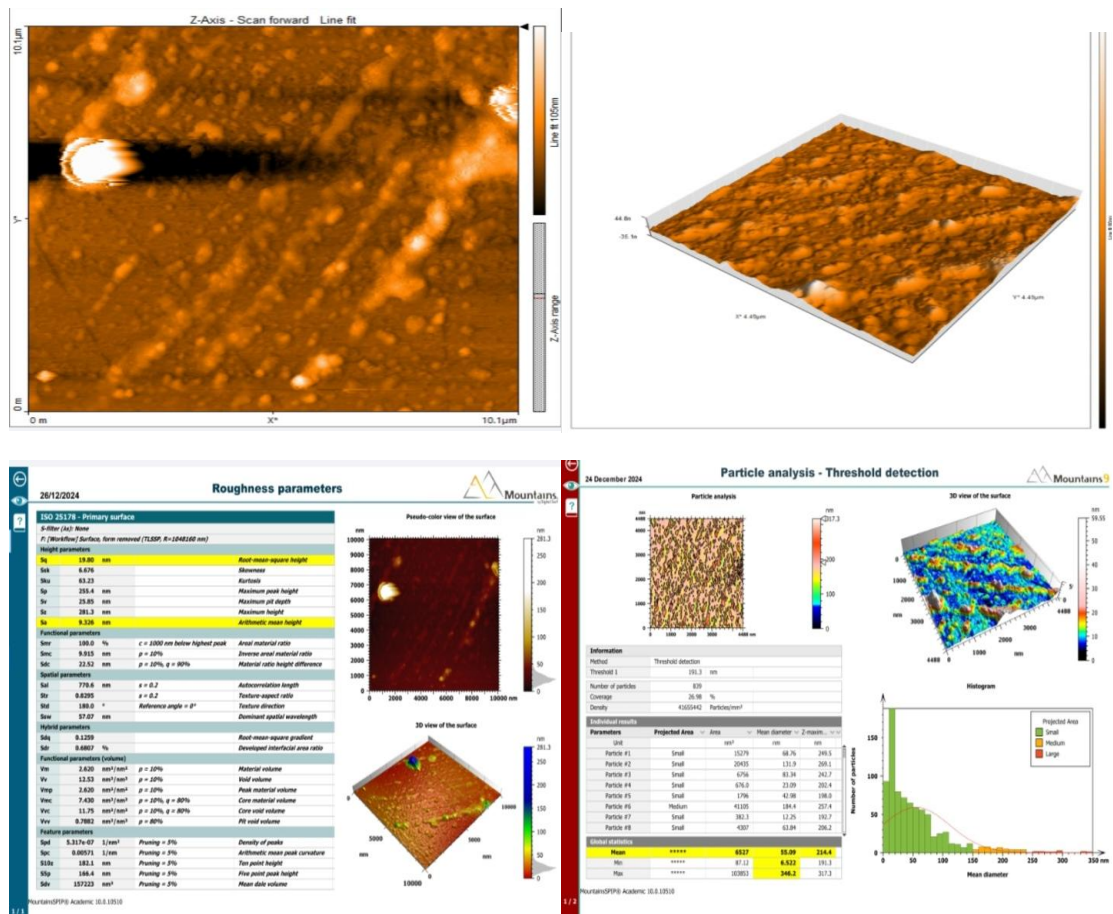


Fig. 3. Topographic characterization and size distribution of nanoparticles on the silicon surface after 2 minutes of plasma etching.



of plasma exposure induce irregular erosion of the native oxide layer, resulting in stochastic roughness as a consequence of the different interaction of ions with surface defects. Etching is not an orderly process at this stage but a ‘revealing’ of the raw silicon surface, which leads to an increase of the initial roughness values. The value of  $aS$  was found to be 21.57 nm. Such a relative increase in roughness with respect to raw silicon ( $qS$ ) confirms the efficiency of DC Jet Plasma in modifying the surface in a record time: one minute.

The value recorded was 2.900. This is a positive value, which means the dominance of peaks on the surface instead of valleys. Physically, this meant plasma did selective etching leaving behind prominent atomic clusters. The kurtality coefficient ( $k_{ku}S$ ) The value reached 15.4 which is very high (since  $k_{ku}S < 3$  indicates a tapered distribution). This suggests very sharp, isolated protrusions that can be used for applications such as electric field focusing or reduction of optical reflectance.

Threshold detection analysis reveals the formation of 387 nanoparticles with numerical density of  $1.26 \times 10^7 \text{ mm}^{-2}$ . The average effective diameter of the particles was 42.24 nm and the maximum height of some peaks was 197.7 nm at nanoscale dimensions. The histogram shows that most of the nanostructures are in the small size range (less than 100 nm), which demonstrates the ability of the utilised technique to produce a rather uniform nanostructured surface even though the ion bombardment is random.

Fig. 3 presents three-dimensional atomic force microscopy (AFM) images of a silicon surface treated with 2-minute argon plasma (DC Jet) showing the formation of nanospikes across the entire scanned area. The surface topography displayed high, pointed protrusions emanating from the base of the surface, signifying a substantial ion sputtering effect on the initial flatness of the surface. Morphologically, the etching process has progressed beyond the initial

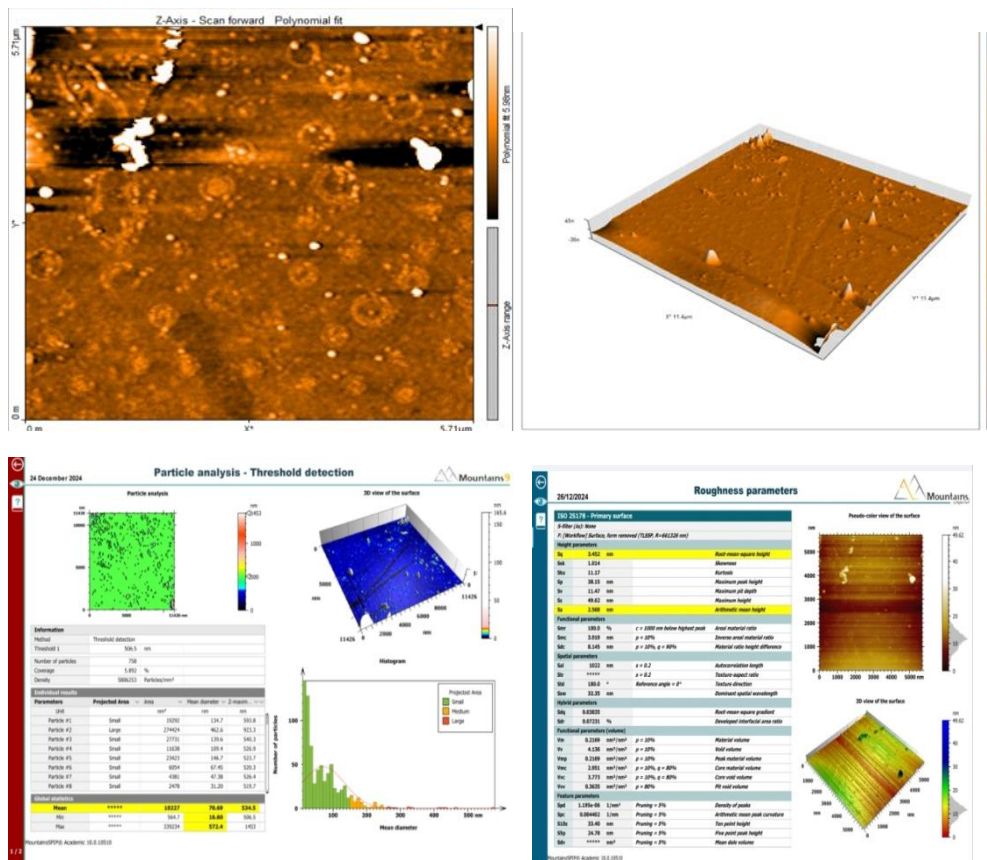


Fig. 4. Topographic characterization and size distribution of nanoparticles on the silicon surface after 3 minutes of plasma etching.

roughening stage to form well-defined vertical nanostructures. The surface topography features prominent sharp protrusions emanating from the surface base, which reflects a strong ion sputtering effect on the original surface flatness. From the morphological appearance it can be seen that the etching process has progressed from the initial roughening stage to the formation of distinct vertical nanostructures. Statistical analysis of the surface showed exact values that reflect the unique geometric properties resulting from two-minute drilling, namely

Parameters of elevation  $a_s$  and  $q_s$ . The arithmetic mean roughness  $a_s$  of the surface was 9.326 nm, and the root mean squared value  $q_s$  was 19.80 nm. These values show that the whole surface develops a relatively fine and regular nano-topography.

The azimuth value is approximately 6.676. This very high positive value is a strong physical indicator of a “peak-heavy” surface, where elevated protrusions dominate the elevation distribution significantly, as opposed to valleys.

The kurtosis value reached a very high value of 63.23. Values greater than 3 in surface topography represent a leptokurtic distribution, i.e. the peaks occurring are very sharp and isolated. This results in unique physical properties of the surface concerning the concentration of electric fields or light scattering. This phenomenon is intimately related to the so-called ‘self-induced micromasking effect’ discussed by Jansen et al [23] The study shows that the accumulation of some sputtered atoms in some places acts as nano-shields to protect the underlying surface from erosion

while the vertical erosion continues around them, leading to very sharp and isolated peaks. The enormous increase in  $k_{ku}S$  supports the “differential erosion” described by Jansen, the surface being in its most sensitive state two minutes out due to the extreme sharpness of the peaks.

The maximum height between the highest peak and deepest valley was found to be 281.3 nm. This confirmed the ability of the plasma to penetrate the surface and create significant changes in height at the nanoscale.

The study area contains 839 particles (protrusions) with an enormous number density of about  $4.16 \times 10^7$  particles per  $mm^2$ .

Surface coverage: The surface coverage of these particles was approximately 26.98%, suggesting that the etching has transformed more than a quarter of the surface area into protruding nanostructures. The average real diameter of these particles was 55.09 nm and the average maximum peak height (z-maximum) was 214.4 nm. The histogram presents a distribution peaked in the small nanoscale, confirming the homogeneity of the nanoscale properties of the engineered surface. When the accelerated positive ions from the argon plasma impinge on it for 2 min, the atoms of the silicon surface are knocked out. The very high values of 63.23  $k_{ku}S$  and 6.676  $s_kS$  suggest that some surface areas showed higher etching resistance (perhaps due to redeposition of some ripped atoms or surface impurities) and acted as fine nanomasks that protected the underlying material from etching, while the surrounding areas continued to erode. This led to the formation of the observed sharp and elongated

Table 1. Comparative Surface Roughness and Particle Analysis Parameters for Silicon Etched by DC Jet Argon Plasma at Different Time Intervals.

Parameter	Units	1 Minute	2 Minutes	3 Minutes	Trend Analysis
Arithmetic Mean Height $a_s$	nm	14.07	9.326	2.568	Continuous Smoothing
Root Mean Square Height $q_s$	nm	21.57	19.80	3.452	Significant Reduction
Skewness $s_kS$	-	2.900	6.676	1.014	Peak-dominated at 2 min
Kurtosis $k_{ku}S$	-	15.43	63.23	11.17	Extreme Spiking at 2 min
Maximum Height $z_s$	nm	197.7	281.3	49.62	Peak at 2 min then collapse
Particle Density	$mm^2$	$1.26 * 10^7$	$4.16 * 10^7$	$0.58 * 10^7$	Nucleation then Coalescence
Mean Particle Diameter	nm	42.24	55.09	70.69	Growth with Etching Time
Surface Coverage	%	14.50	26.98	5.892	Maximum efficiency at 2 min



the plasma to induce a full surface nanopolishing process at this treatment time.

The value was 1.014, a positive value confirming the continued preponderance of peaks to valleys in the surface elevation profile, and thus supporting the hypothesis of prominent protrusions above the smoothed base level. The kurtosis coefficient ( $k_{ku}$ ) was 11.17, which was much higher than the standard value (3), indicating a “highly pointed” (leptokurtic) surface elevation distribution. Physically this implies that the surface, while being overall smooth as demonstrated by the low aS-value, still shows very sharp and isolated protrusions.

The maximum elevation difference between the highest peak and the deepest valley reached 49.62 nm, which shows the subtle local variation of surface topography. A threshold detection analysis showed that the nanostructures were created in a dense and well defined distribution, in terms of density and number: 758 nanoparticles

(protrusions) were identified in the study area with a numerical density of  $5.80 \times 10^6$  particles/mm<sup>2</sup>.

The average actual diameter of these particles was 70.69 nm. Interestingly, the average maximum height (Max Z) of these particles was 534.5 nm, with some maximum heights reaching 1453 nm at some points thanks to the dominance of the ion polishing mechanism during the 3 min treatment time. The continuous bombardment with high kinetic energy argon ions (Ar<sup>+</sup>) removes large surface irregularities and smoothens the random topography which accounts for the significant decrease in the value of aS. Simultaneously, the phenomenon of self-masking is very important. Some of the particles that have been drilled out and redeposited act as nanoshields protecting the areas below from vertical drilling. This leads to extremely sharp and elongated nano-protrusions (High Aspect Ratio). It is this interplay of global polishing and selective protected drilling that gives rise to this surface, which is extremely smooth

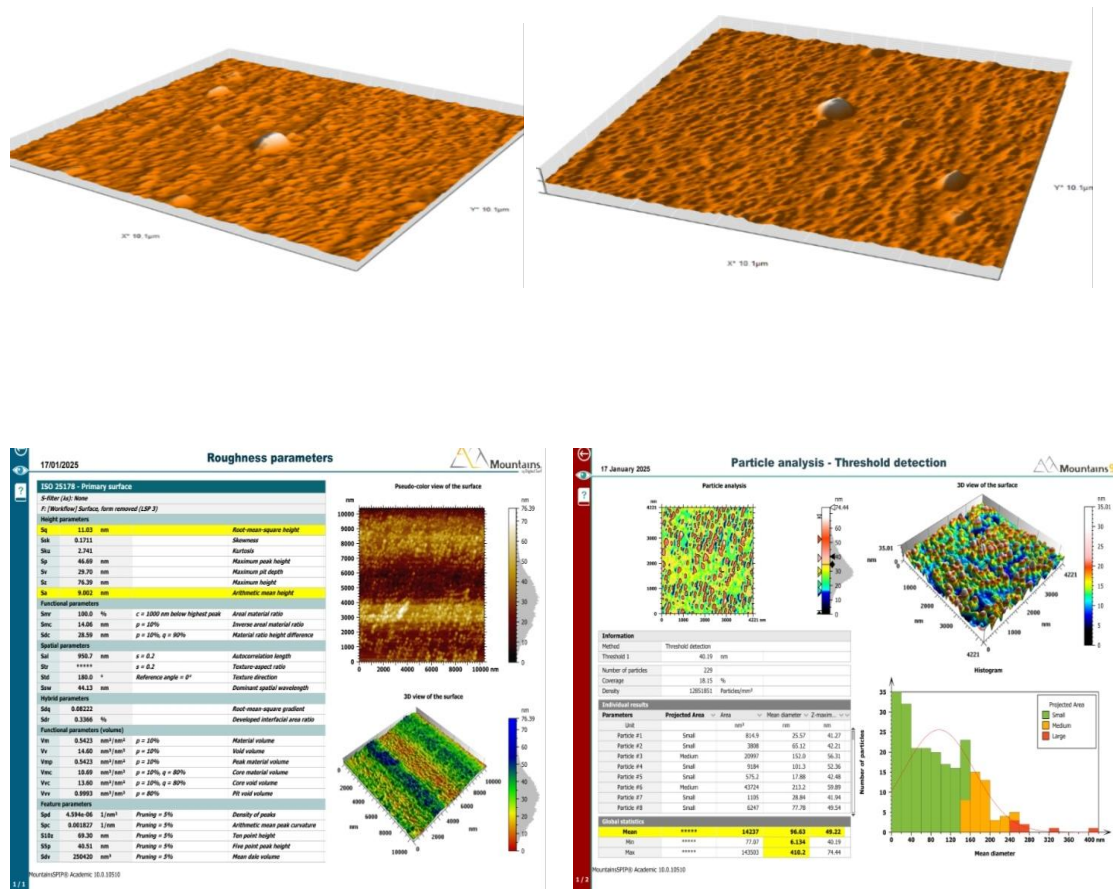


Fig. 6. Topographic characterization and size distribution of nanoparticles on the silicon surface after 2 minutes of wet etching.

and yet features protrusions with remarkable sharpness.

A Chemical etching for one-minute results in a surface roughness  $a_s = 7.15$  nm) and a root mean square height ( $q_s = 8.44$  nm). This behaviour is due to the chemical reaction of KOH with the silicon crystal, which is called “anisotropic etching”. The KOH solution attacks the silicon atoms at different rates depending on the atomic density of the crystal planes, where the etching rate in the  $\langle 100 \rangle$  direction is much faster than in the  $\langle 111 \rangle$  direction [25]. This variation leads to the appearance of regular geometric structures (such as truncated pyramids or grooves) rather than random protrusions.

The surface showed a positive symmetry value  $S_{sk}$  and kurtosis value  $S_{ku} = 3.69$ . The kurtosis value close to 3 suggests that the elevation distribution is close to a Gaussian distribution with relatively stable, broad-based protrusions [26]. This suggests that one minute of KOH etching was sufficient to remove the surface layer and form regular microstructure “seeds”, but it was not yet sufficient to have a high needle sharpness as in other etching techniques, such as plasma etching. These results were in agreement with the study by Pal et al. (2021) [26] which confirmed that the initial stages of KOH etching of silicon lead to the formation of topography that is mainly dependent on surface chemistry and provides

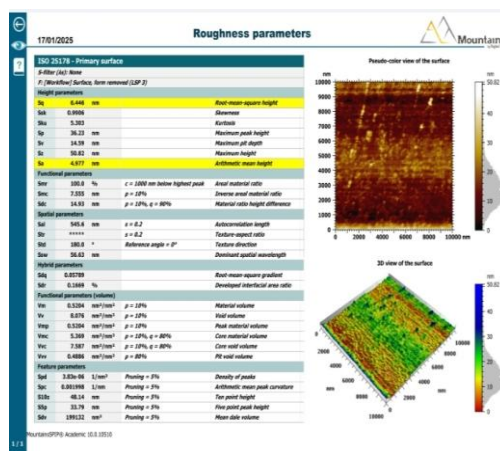
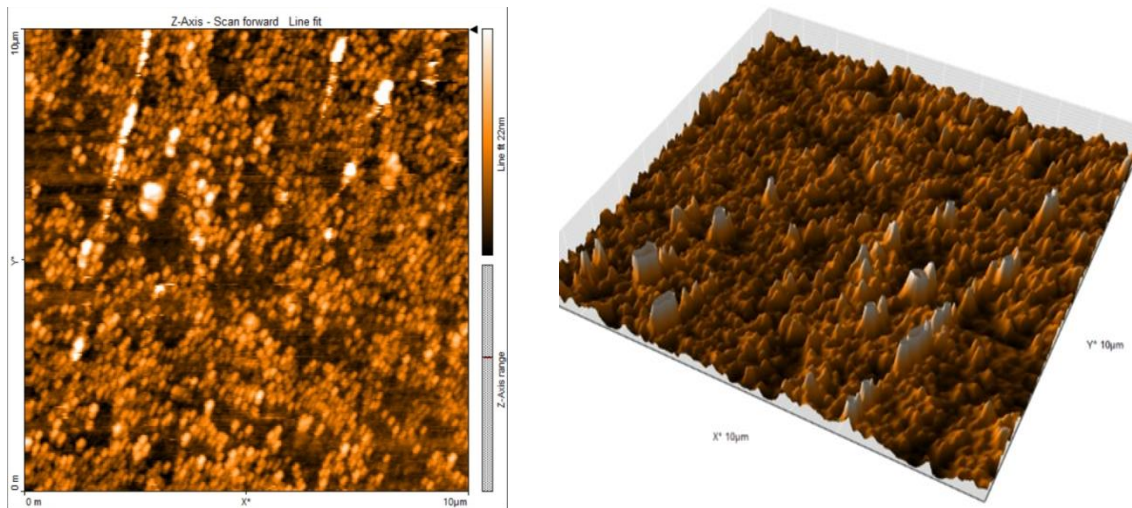


Fig. 7. Topographic characterization and size distribution of nanoparticles on the silicon surface after 3 minutes of wet etching.

active sites for reaction, thus paving the way for an increased effective surface area [21]. The value of the kurtosis 3 shows that the distribution of the elevation is tending to the distribution of Gaussian with relatively stable and broad-based protrusions [27]. This means that one minute etching with KOH was enough to remove the surface layer and to form the regular microstructure seeds. But it was not yet the high needle sharpness which can be found in other etching techniques like plasma etching. These results are in accord with the study by Pal et al. (2021) [26] where it was confirmed that the initial steps of KOH etching of silicon result in topography formation which is predominantly governed by surface chemistry and provides active sites for reaction which in turn leads to the enhancement of the effective surface area [21].

The atomic force microscopy (AFM) analysis of the silicon surface after exposure to potassium hydroxide (KOH) solution for two minutes reveals a strong alteration of the nanostructure compared to one minute exposure. The etching time increase to two minutes leads to higher mean roughness (Sa) and root mean square (Sq) values. The increase indicates that the chemical etching process penetrates deeper into the silicon crystalline planes. As the chemical reaction proceeds, nanopyrramids begin to grow and merge. Since the KOH solution etches the  $100^\circ$  direction much faster than the  $111^\circ$  direction, the slower-etched crystalline planes become more pronounced, increasing the contrast between the peaks and valleys on the surface [21]. The mean roughness (Sa) and root mean square (Sq) values were increased further with the etching time was increased to two minutes. Such increase indicates that the chemical etching process is going deeper to the planes of silicon crystals. As the chemical reaction progresses, the nanopyrramids start growing and merging. The KOH solution etches the crystalline plane of  $100^\circ$  direction much faster than the  $111^\circ$  direction so the crystalline plane of the slower etching becomes more prominent and the contrast between the peaks and the valleys of the surface increases [21].

The results suggest that the kurtosis value  $_{ku}S$  is gradually deviating from the number (3) and the symmetry value  $_{sk}S$  is positive. Discussion: The increase of the value of  $_{ku}S$  indicates that the surface begins to have more "sharpness" on the peaks of the created pyramidal structures compared to the first minute. The distribution of the heights

shows that the peaks are more dominant than the valleys. This development is in agreement with the results of Zubel et al. (2012) who pointed out that the morphology of silicon etched with KOH passes through a transitional phase between one and two minutes in which the random topography begins to disappear and is replaced by regular geometric structures with specific angles of inclination that match the crystal planes [28]. The sample etched for two minutes is more efficient in function than the one-minute sample. Discussion: The increase of the value of  $_{ku}S$  indicates that the surface started to be more sharp at the tops of the resulting pyramidal structures than the first minute. The distribution of the elevation evidences that there are more dominant peaks than valleys. This result is in agreement with the results obtained by Zubel et al. (2012) who showed that the morphology of KOH etched silicon is in a transitional state between one and two minutes, when the random topography begins to disappear and is replaced by regular geometrical structures with certain angles of inclination which correspond to the crystal planes [28]. The two-minute etched sample is functionally more effective than the one-minute sample

The 3 min etching time was a stabilisation and integration step of the nanostructures on the silicon surface. AFM data revealed qualitative changes in topographical parameters when compared to previous times (1 and 2 min):

The surface showed the highest values of mean roughness (Sa) and maximum peak height at this time. This continued growth shows that the KOH solution was able to penetrate the surface silicon layers where the nanopyrria became more prominent and penetrated deeper. At this stage, the maximum depth of the grooves separating the peaks is reached, which indicates the high selectivity of the KOH solution for different crystalline planes [1]. Instead of just increasing the number of protrusions, we see a "volumetric growth" of the existing structures, where small peaks merge into larger and more stable pyramidal structures. This explains the increase in the value of Sq (root mean squared), which is sensitive to large deviations in altitude. At 3 minutes we see the kurtosis coefficient ( $_{ku}S$ ) and the symmetry coefficient ( $_{sk}S$ ) to tend to stability or slight change towards a more "equilibrium" structure. This result agrees with the study of Tan et al. (2017) [29] where a chemical etching time of 3 minutes

was used for a “morphological equilibrium” state, in which the nanopyramids are tightly packed to fill the initial plane.

## CONCLUSION

The work reveals that the dynamic mechanisms controlling the morphological evolution of Si surfaces are different for physical and chemical etching processes, which allows for high-precision nanosurface engineering for various technological applications. Quantitative analysis based on the ISO 25178 standard has revealed that the etching of plasma of argon (DC Jet Plasma) is characterised by a nonlinear course described by the Bradley-Harper theory. At 2 minutes, ion-induced roughening mechanisms dominated, resulting in the formation of extremely sharp needle-like structures (nanospikes) with the highest kurite values  $k_{ku}$  before surface diffusion processes took over at 3 minutes, leading to ion polishing and peak flattening. On the other hand, the chemical etching using KOH solution showed structured and cumulative behaviour under crystal selectivity (anisotropic etching), which resulted in steady and progressive growth of nanopyramid structures. These structures increased in geometry and roughness ( $S_a$ ) with the curing time, without reaching a smoothing stage. This comparison validates that plasma etching is the most powerful tool to produce surfaces with a sharp concentrated topography ( $\lambda$ ) at critical times, and that chemical etching is a strategic option to produce surfaces with a homogeneous surface energy distribution and regular geometries. These results provide a complete framework for the understanding of the control of the silicon topography at the nanoscale, opening the way for the design of a new generation of silicon-based electronic and optoelectronic platforms by choosing the best etching technique and the time of the process to reach the topography properties of interest.

## CONFLICT OF INTEREST

The authors declare that there is no conflict of interests regarding the publication of this manuscript.

## REFERENCES

1. Sze SM, Ng KK. *Physics of Semiconductor Devices*: Wiley; 2006 2006/04/10.
2. Fifiis P, Christenson MP, Connolly N, Ruzic DN. Nanostructuring of Palladium with Low-Temperature Helium Plasma. *Nanomaterials*. 2015;5(4):2007-2018.
3. Canham L. Porous Silicon Membranes. *Handbook of Porous Silicon*: Springer International Publishing; 2014. p. 1-7.
4. Lieberman MA, Lichtenberg AJ. *Principles of Plasma Discharges and Materials Processing*: Wiley; 2005 2005/01/27.
5. Makeev MA, Cuerno R, Barabási A-L. Morphology of ion-sputtered surfaces. *Nuclear Instruments and Methods in Physics Research Section B: Beam Interactions with Materials and Atoms*. 2002;197(3-4):185-227.
6. Bradley RM, Harper JME. Theory of ripple topography induced by ion bombardment. *Journal of Vacuum Science and Technology A: Vacuum, Surfaces, and Films*. 1988;6(4):2390-2395.
7. Cuerno R, Barabási A-L. Dynamic Scaling of Ion-Sputtered Surfaces. *Phys Rev Lett*. 1995;74(23):4746-4749.
8. Valbusa U, Boragno C, Mongeot FBd. Nanostructuring surfaces by ion sputtering. *J Phys: Condens Matter*. 2002;14(35):8153-8175.
9. Muñoz-García J, Vázquez L, Cuerno R, Sánchez-García JA, Castro M, Gago R. Self-Organized Surface Nanopatterning by Ion Beam Sputtering. *Toward Functional Nanomaterials*: Springer US; 2009. p. 323-398.
10. Huang J, Wan Q. Gas Sensors Based on Semiconducting Metal Oxide One-Dimensional Nanostructures. *Sensors*. 2009;9(12):9903-9924.
11. Khlebtsov B, Khlebtsov N. Surface-Enhanced Raman Scattering-Based Lateral-Flow Immunoassay. *Nanomaterials*. 2020;10(11):2228.
12. Righettoni M, Amann A, Pratsinis SE. Breath analysis by nanostructured metal oxides as chemo-resistive gas sensors. *Mater Today*. 2015;18(3):163-171.
13. Mandracci P, Rivolo P. Recent Advances in the Plasma-Assisted Synthesis of Silicon-Based Thin-Films and Nanostructures. MDPI AG; 2023.
14. Geometrical product specifications (GPS) - Surface texture: Profile. BSI British Standards. <http://dx.doi.org/10.3403/bseniso21920>
15. Luo X, Zhang Z, Chen L, Xiong Y, Shu Y, He J, et al. The near-surface microstructural evolution and the influence of Si particles during nanoscratching of nanocrystalline Al. *Appl Surf Sci*. 2022;573:151533.
16. Sigmund P. Theory of Sputtering. I. Sputtering Yield of Amorphous and Polycrystalline Targets. *Phys Rev*. 1969;184(2):383-416.
17. Coburn JW, Winters HF. Ion- and electron-assisted gas-surface chemistry—An important effect in plasma etching. *J Appl Phys*. 1979;50(5):3189-3196.
18. Petersohn D. *Principles of plasma discharges and materials processing*. Von. M. A. Liebermann und A. J. Lichtenberg, XXVI, 572S., John Wiley and Sons, Inc., New York 1994, £ 54.00, ISBN 0-471-00577-0. *Mater Corros*. 1995;46(9):551-551.
19. Chapman B, Vossen JL. *Glow Discharge Processes: Sputtering and Plasma Etching*. *Phys Today*. 1981;34(7):62-62.
20. Franssila S. *Introduction to Microfabrication*: Wiley; 2010 2010/09/17.
21. Madou MJ. *Fundamentals of Microfabrication and Nanotechnology, Three-Volume Set*. CRC Press; 2018.
22. Yamada I. Surface modification and other advanced ion beam processing projects in Japan. *Surf Coat Technol*. 1992;51(1-3):514-521.
23. Jansen HV, de Boer MJ, Unnikrishnan S, Louwse MC,

- Elwenspoek MC. Black silicon method: X. A review on high speed and selective plasma etching of silicon with profile control: an in-depth comparison between Bosch and cryostat DRIE processes as a roadmap to next generation equipment. *Journal of Micromechanics and Microengineering*. 2009;19(3):033001.
24. Xiao H, Dai Y, Duan J, Tian Y, Li J. Material removal and surface evolution of single crystal silicon during ion beam polishing. *Appl Surf Sci*. 2021;544:148954.
25. Seidel H, Csepregi L, Heuberger A, Baumgärtel H. Anisotropic Etching of Crystalline Silicon in Alkaline Solutions: I. Orientation Dependence and Behavior of Passivation Layers. *J Electrochem Soc*. 1990;137(11):3612-3626.
26. Transient Clustering of Reaction Intermediates during Wet Etching of Silicon Nanostructures. American Chemical Society (ACS). <http://dx.doi.org/10.1021/acs.nanolett.7b00196.s002>
27. Geometrical product specifications (GPS) Surface texture: Areal. BSI British Standards. <http://dx.doi.org/10.3403/bseniso25178>
28. Zubel I, Kramkowska M. The effect of isopropyl alcohol on etching rate and roughness of (1 0 0) Si surface etched in KOH and TMAH solutions. *Sensors and Actuators A: Physical*. 2001;93(2):138-147.
29. Zimmer K, Böhme R. Precise etching of fused silica for micro-optical applications. *Appl Surf Sci*. 2005;243(1-4):415-420.